Babeş-Bolyai University
Faculty of Physics

# Scientific Report for Project
# PN-II-RU-TE-2014-4-2360

## January - September 2017

Project Director: Dr. Albert Takacs

September 2017

## Contents

# 1. Project Objectives

This project intends to approach the study of the exchange spring concept in thin films experimentally as well as theoretically. An important aspect is the dimensionality effect, the variation of magnetic moments at surfaces and interfaces being correlated with magnetic anisotropy. Therefore, the influence of the deposition conditions of both hard and soft magnetic films is important in order to successfully prepare and investigate exchange coupled multilayer films. The project has two main objectives.

The first objective is focused on the preparation and study of hard and soft magnetic films. The effects of preparation conditions on the structural, microstructural and magnetic properties of hard and soft magnetic films will be investigated (Ar pressure, deposition temperature, sputtering power, substrate type, substrate thickness, and film thickness). Fully relativistic band structure calculations will also be employed in order to have a clear input for the experimental part of the project.

The second objective proposes the preparation and study of exchange coupled multilayer systems based on the results obtained after accomplishing the first objective. $SmCo_5/Fe_{65}Co_{35}/SmCo_5$ multilayer films are to be prepared, in which the easy magnetization axis of both hard magnetic layers is aligned along one single direction. The interlayer exchange coupling will be studied by hysteresis measurements and by DC-demagnetizing loops for different thicknesses of the soft magnetic thin film. In order to support the experimental observations, electronic structure calculations will also be performed. A successful coupling together with the optimum texture provided by the epitaxial growth of the hard magnetic thin film would lead to excellent magnetic properties. We are aiming for small thicknesses for the soft magnetic material (raging from a few nm) in order to get fully coupled layers. Hysteresis curves with high coercivity and large remanence are expected.

# 2. Phase 3: January - September 2017

## 2.1. Results Summary for Phase 3: January - September 2017

In this section, we will present the results of the project for the period January - September 2017. In Phase 3 we continued the study of the structural properties of Cr/$SmCo_5$/Cr films and focused our attention on investigating the magnetic properties of exchange coupled hard/soft magnetic multilayers. The obtained results were submitted for publication in ISI and BDI indexed articles [1, 2] and presented at international conferences [3-8]. A bachelor thesis was successfully completed on the project theme. In subsection 2.1.1 we discuss the effect of substrate type (glass, Si) and deposition parameters (substrate temperature, Ar pressure) on the structural properties of Cr/Sm-Co multilayers. In subsection 2.1.2, we present the effect of $Fe_{65}Co_{35}$ layer thickness on the magnetic properties of exchange coupled hard/soft Cr/$SmCo_5$/$Fe_{65}Co_{35}$/$SmCo_5$/Cr multilayers.

### 2.1.1. Effect of Substrate Type and Deposition Parameters on the Structural Properties of Cr/Sm-Co/Cr Thin Films

The investigation of the effect of the Ar pressure, substrate temperature and substrate type on the crystal structure of the hard magnetic phase represents a step forward in the development of thin films with magnetic properties. By varying these two parameters, the complexity of the Sm-Co phase can be triggered. A Cr buffer layer represents a proper base for growing Sm-Co. Also, the Cr layer prevents the Sm atoms from interacting with the oxidized Si substrate. A large magnetocrystalline anisotropy has been found in the $SmCo_5$ phase [8]. By varying the pressure in the process of deposition the crystal structure of the hard magnetic thin film can be influenced. In the case of epitaxial growth, the deposited atoms grow in registry with the substrate due to atomic bonding. Epitaxial growth tends to occur when the lattice mismatch between the substrate and the deposited materials is small.

The formation of the texture of a thin film is strongly influenced by the three main sputtering conditions that can be varied, which are represented by the substrate temperature, the Ar pressure and sputtering power [10, 11]. The dependence of the crystal structure and texture on the substrate temperature can be explained by taking into consideration the influence that the mobility and kinetic energy of the adatoms has on the nucleation of islands [11]. The mobility of the adatoms can be increased if the substrate temperature is increased and this can lead to a higher surface diffusion. On the other hand, a lower substrate temperature can lead to the formation of smaller islands with a random orientation [11]. The change in the sputtering power affects the deposition rate and also the

kinetic energy of the bombarding atoms, which leads to the change in the nucleation and growth of the thin film [11]. The influence that the Ar pressure has on the crystallographic texture is related to the influence that the Ar pressure has on the kinetic energy of the deposited atoms. If the Ar pressure is increased, the average kinetic energy of the deposited atoms decreases. This is a consequence of the collisions that take place between the deposited atoms and the Ar ions [11].

The film deposition was made using DC magnetron sputtering. The thin films were deposited as multilayer samples consisting of Cr(100nm)/Sm-Co(100 nm)/Cr(5 nm). The Cr underlayer is used as a buffer layer between the substrate and the Sm-Co layer. The Cr buffer layer prevents the oxygen diffusion from the substrate into the Sm-Co layer and also ensures that the SmCo layer grows in tune with the underlayer. The Cr capping layer protects the SmCo layer from atmospheric oxidation. The base pressure was around $10^{-7}$ mbar. For the Cr buffer and capping layers, the Ar partial pressure was kept at 3.5 mtorr and the sputtering power was kept at 30 W. For the $SmCo_5$ layer the Ar partial pressure was kept constant at 1, 2, 3, 5 and 7 mtorr respectively. The deposition power for the $SmCo_5$ layers was 90 W. For the Cr underlayer the substrate was kept at room temperature while for the $SmCo_5$ layer and the Cr capping layer the substrate temperature was kept at room temperature and 500 ºC respectively. The film thickness and deposition rate was monitored in situ using an Inficon SQM-160 rate/thickness monitor previously calibrated by X-ray reflectivity.

X-ray diffraction measurements were performed using a Bruker D8 Advance diffractometer using Cu $K_\alpha$ radiation and Bragg-Brentano focusing geometry. Measurements were performed as θ-2θ scans for the samples deposited on $Si/SiO_2$ between 20 and 60 degrees with a step of 0.02 degrees. For the samples deposited on glass the XRD measurements were performed as 2θ detector scans while the source θ was kept fixed at 10º. During the measurements, the samples were rotated along the out of plane φ axis.

In order to investigate the effect of the substrate we used Corning cover glass and Si (100) coated with 100 nm Si oxide. For studying the effect of substrate temperature two sets of samples were deposited, one with a substrate at room temperature and one with a substrate temperature of 500 ºC. Each sample set was deposited as Cr/Sm-Co/Cr samples at different pressures ranging from 1 to 7 mtorr. The effect of annealing was also studied on the deposited samples by subjecting the films to a thermal treatment at 600 ºC for 1 hour (Si substrates). Annealing was performed in sealed quartz tubes and resistive furnaces. The pressure during the annealing was better than $10^{-6}$ mbar.

The X-ray diffraction patterns for the Cr/Sm-Co/Cr samples as-deposited at room temperature on Corning glass at different pressures are illustrated in Figure 1. The XRD patterns are noisy, more specifically they have a low signal to noise ratio due to the fact that

the glass substrates are amorphous and the layers are thin compared to the substrate. The X-ray beam penetrates the samples around 1-10 μm, therefore the X-ray will pass through 0.1 μm of film and 0.9 to 10 μm of substrate. Only a small portion of the diffracted beam will carry information about the film while the rest of the beam carries information about the substrate. This leads to a small signal to noise ratio, i.e. a noisy diffraction pattern. The XRD patterns show a very broad, large peak at low angles ($2\theta < 30^{o}$) which originates from the glass substrates.

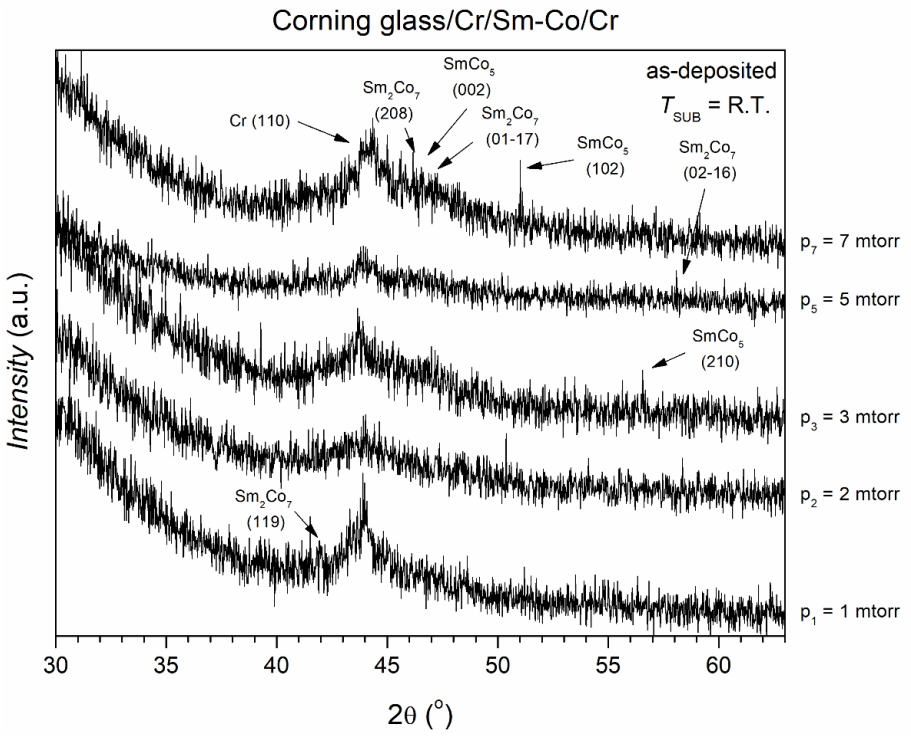


**Figure 1.** The X-ray diffraction patterns for the Cr/Sm-Co/Cr samples deposited on Corning glass at room temperature and Ar pressures of 1, 2, 3, 5 and 7 mtorr.

The XRD patterns show the presence of a broad Cr (110) peak in all of the samples. The broadness of the Cr (110) peaks points to the presence of strain in our samples which could be explained by the fact that the glass substrate is amorphous. Texturing along the (110) direction has been previously shown in Cr films deposited on glass substrates at room temperature and low sputtering power. Also, it was previously shown that Cr films texture along the (110) direction for Ar pressures up to 10 mtorr [11]. Taking into account the fact that we deposited the Cr underlayer at room temperature, low power and Ar pressure below 10 mtorr we can safely deduce that the Cr underlayer in our samples is textured along the (110) direction.

The XRD pattern of the Cr/Sm-Co/Cr sample deposited at the pressure of 1 mtorr shows only a very faint (110) peak of the $Sm_2Co_7$ phase. No other peaks belonging to either

$SmCo_5$, $Sm_2Co_7$ or $Sm_2Co_{17}$ were identified, leading us to believe that the Sm-Co layer is mostly amorphous. While the glass substrate is amorphous, the Cr underlayer is crystalline which would lead us to the assumption that the $SmCo_5$ layer would also be crystalline, however, the results show this is not the case. Cr has a BCC unit cell and a lattice parameter of 2.88 Å, while $SmCo_5$ is hexagonal and has lattice parameters *a* = 5 Å and *c* = 3.96 Å [12], therefore there is a rather large mismatch between the two unit cells and this can lead to a uncontrolled growth of the Sm-Co layer and a high degree of strain in the film. Because the deposition of the Sm-Co layer was made at room temperature, the Sm-Co adatoms do not have sufficient kinetic energy in order to promote surface diffusion therefore the atoms are quenched when they reach the surface. The effect of these parameters (substrate mismatch, temperature) on the crystal structure of the deposited film, which was explained above, could explain the absence of the Sm-Co peaks or their very low intensity in the sample deposited at the pressure of 1 mtorr. The same behavior was found for the sample deposited at 2 mtorr.

The samples with Sm-Co layers deposited at higher Ar pressures (3-7 mtorr) show XRD peaks corresponding to the $SmCo_5$ or $Sm_2Co_7$ phases, showing that the Sm-Co layers are phase mixtures. The sample deposited at 3 mtorr shows the $SmCo_5$ (210) peak and the $SmCo_5$ (002), $Sm_2Co_7$ (208) and $Sm_2Co_7$ (01-17) peaks. However, only the $SmCo_5$ (210) peak can be clearly identified. The $SmCo_5$ (002), the $Sm_2Co_7$ (208) and $Sm_2Co_7$ (01-17) overlap forming a very broad peak next to the Cr (110) peak and cannot be distinguished from each other. By increasing the Sm-Co deposition pressure to 5 mtorr only the $Sm_2Co_7$ (02-16) peak is present. The sample with the Sm-Co layer deposited at an Ar pressure of 7 mtorr shows the peaks corresponding to $SmCo_5$ (210), $SmCo_5$ (002), $Sm_2Co_7$ (208) and $Sm_2Co_7$ (01-17) along with an intense $SmCo_5$ (102) peak. This shows that the phase of interest, $SmCo_5$, is formed, however the sample contains the $Sm_2Co_7$ impurity phase.

The $Sm_2Co_7$ phase is also a hexagonal phase and its unit cell is derived from the $SmCo_5$ crystal structure by replacing some Co atoms with Sm atoms followed by layer shifts and minor rearrangements [13, 14]. Therefore, the formation of $Sm_2Co_7$ phase in our samples could be attributed to the fact that $SmCo_5$ is metastable below 1023 K and it usually decomposes into a mixture of $Sm_2Co_7$ and $Sm_2Co_{17}$. The behavior described above can be explained by the effect of Ar pressure during deposition on the crystal structure, texturing and stoichiometry of the Sm-Co layer. First the behavior must be analyzed in terms of kinetic energy. At low Ar pressure the Sm and Co atoms coming from the target towards the substrate face a small amount of collisions with the Ar ions therefore there should be no change in stoichiometry of the film compared to the target. As the Sm and Co atoms bombard the surface, some of their kinetic energy can convert into thermal energy causing them to diffuse along the surface. Depending on their kinetic energy and consequently their

surface diffusion energy, the $SmCo_5$ layer can texture along different directions. As texturing implies the preferential orientation of one or more atomic planes over other planes it is possible that some reflections will be absent from the X-ray diffraction pattern. Therefore, there are two possible explanations for the absence of $SmCo_5$ peaks in the as-deposited samples prepared at 1 and 2 mtorr. A first possible explanation would be that the Sm-Co layers are amorphous, as explained above. A second explanation could be that the Sm-Co layer is textured along a certain direction, however the limitations imposed by the measurement techniques do not allow the observation of the reflections characteristic to the texture. Because the measurement interval is rather narrow (30º - 60º) and the signal to noise ratio is poor, in conjunction with the lower intensity of Sm-Co reflections due to strain could cause the apparent absence of $SmCo_5$ peaks in the XRD pattern.

Increasing the Ar pressure leads to two effects. A first effect is a loss of energy due to collisions of the Sm and Co atoms with the Ar ions. This leads to a lowering of the kinetic energy of the Sm-Co atoms when they reach the surface, possibly inducing different degrees of texturing. The second effect is the variation of stoichiometry, because even though the Sm and Co atoms suffer collisions, they suffer collisions at different rates, as their atomic radii, and consequently their effective scattering cross-sections are different. This can lead to a

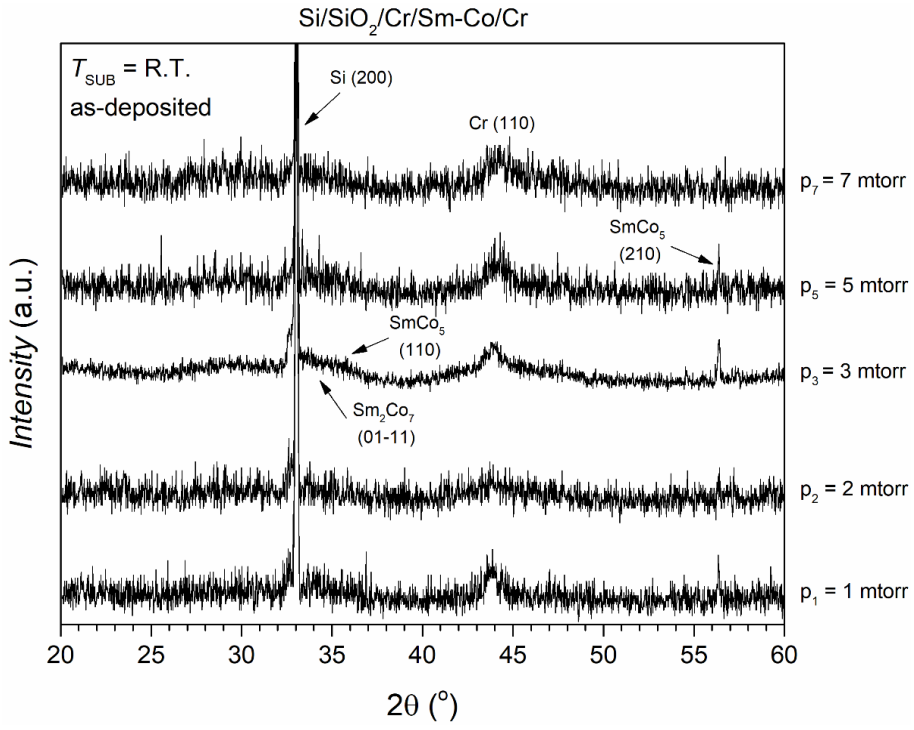


**Figure 2.** The X-ray diffraction patterns for the Cr/Sm-Co/Cr samples deposited on Si(100)/$SiO_2$ at room temperature and Ar pressures of 1, 2, 3, 5 and 7 mtorr.

different number of Sm and Co atoms reaching the substrate surface compared to the target leading to a variation of the layer stoichiometry. This second effect could explain the behavior of the samples deposited at 3-7 mtorr.

The XRD patterns of Cr/Sm-Co/Cr deposited on $Si/SiO_2$ at room temperature and Ar pressures of 1, 2, 3, 5 and 7 mtorr are shown in Figure 2. The XRD patterns show a Si (200) peak and a broad Cr (110) peak. The very intense peak in the diffraction pattern given by the Si (200) reflection, theoretically cannot be observed, however it shows up in the XRD pattern due to the crystal damage which occurs at the edge of the substrate when it is cut. All of the samples show the Cr (110) peak which is an indicative of sample texture, similar to the samples that were deposited on Corning cover glass. In this case the Cr peaks are wide and are similar to the Corning glass case, an indicative of strain induced by the mismatch between Cr and the $SiO_2$ layer in the substrate which was found to be α-cristobalite and is an allotropic form of quartz [15]. At the pressure of 1 mtorr only the $SmCo_5$ (210) peak is visible pointing to the texturing of $SmCo_5$ along this direction. The same texturing was found for Ar pressures for 2, 5 and 7 mtorr. The sample deposited at an Ar pressure of 3 mtorr shows the $SmCo_5$ (210) peak along with a broad shoulder-like peak next to the Si (200) peak which could be attributed to $SmCo_5$ (110), however, given the broadness of the peak it is possible that the $Sm_2Co_7$ (01-11) peak is also present meaning that in this sample we have a phase mixture between $SmCo_5$ and $Sm_2Co_7$. The highest $SmCo_5$ (210) peak intensity was obtained from the sample deposited at 5 mtorr while for samples deposited at 1, 2 and 7 mtorr the intensity of this peak is weaker which could point to a reduced crystallinity of the $SmCo_5$ phase in this sample. From these results, we can infer that the optimum deposition pressure is 5 mtorr.

Compared to the Corning glass case, for samples deposited on $Si/SiO_2$ we obtained very different results. These differences could be attributed to the fact that the $SiO_2$ underlayer in this case is crystalline as opposed to the case of Corning glass. The crystallinity of the $SiO_2$ underlayer could lead to reduced strain in the Cr layer which in turn could lead to a better crystallization of the $SmCo_5$ phase. $SmCo_5$ was reported to have a recrystallization temperature of around 450 ºC. In order to reduce strain in our samples and promote a better crystallization of the $SmCo_5$ phase, the samples deposited at room temperature were annealed in vacuum at 600 ºC for 1 hour. The XRD patterns of the annealed Cr/Sm-Co/Cr deposited on $Si/SiO_2$ at room temperature and Ar pressures of 1, 2, 3, 5 and 7 mtorr is shown in Figure 3. After annealing, the Cr (110) and $SmCo_5$ (210) peaks become narrow and better defined. However, following annealing the samples decompose into a mixture of either $SmCo_5$ and $Sm_2Co_7$ phases ($p$ = 1 - 5 mtorr) or $SmCo_5$, $Sm_2Co_7$, and $Sm_2Co_{17}$ ($p$ = 7 mtorr).

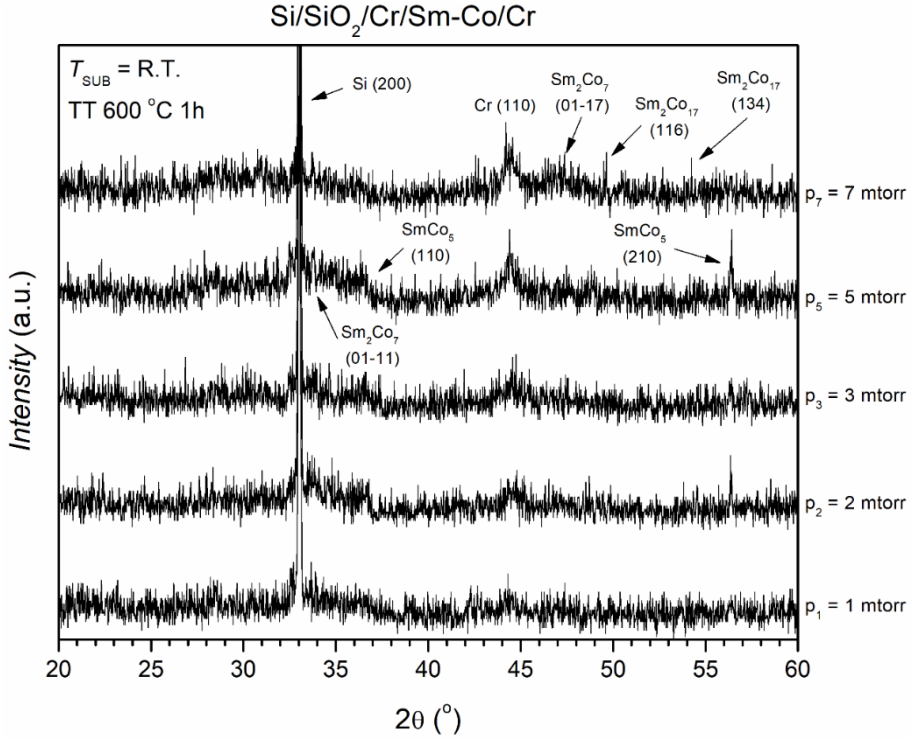


**Figure 3.** The X-ray diffraction patterns for the Cr/Sm-Co/Cr samples deposited on Si(100)/$SiO_2$ at room temperature and Ar pressures of 1, 2, 3, 5 and 7 mtorr, annealed at 600 ºC for 1h.

The effect of substrate temperature was also studied. The XRD patterns for the Cr/Sm-Co/Cr Si deposited at Ar pressures of 1, 2, 3, 5 and 7 mtorr and a substrate temperature of 500 ºC is shown in Figure 4. The samples show the Cr (110) peak similar to the previous samples. The sample deposited at 1 mtorr shows a faint $SmCo_5$ (210) peak along with a wide $Sm_2Co_7$ (019) peak. The sample deposited at 3 mtorr shows only the $Sm_2Co_7$ phase while the sample deposited at 5 mtorr shows only the $SmCo_5$ phase. Surprisingly, the sample deposited at 7 mtorr shows no identifiable Sm-Co peaks. The absence of SmCo peaks at a pressure of 7 mtorr could be explained by a possible lower kinetic energy of the Sm-Co adatoms which could texture the layer in such a way that is not observable in the XRD pattern.

Figure 5 shows the XRD patterns for the Cr/Sm-Co/Cr Si deposited at a substrate temperature of 500 ºC and Ar pressures 1, 3, 5 and 7 mtorr, after annealing at 600 ºC for 1 hour. In this case annealing leads to a narrowing of the Cr peaks, improving the crystallinity of the Cr buffer layer. Unfortunately, annealing leads to a decomposition of the $SmCo_5$ phase into a mixture of $SmCo_5$ and $Sm_2Co_7$ phases, in agreement with the phase diagram.

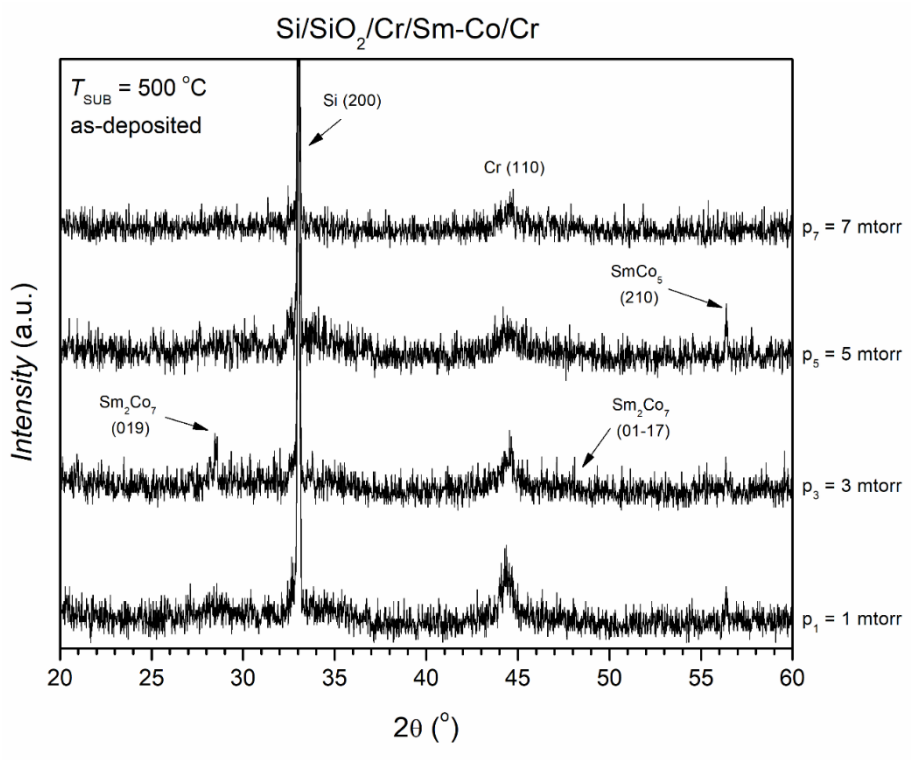


**Figure 4.** The X-ray diffraction patterns for the Cr/Sm-Co/Cr samples deposited on Si(100)/$SiO_2$ at a substrate temperature 500 ºC and Ar pressures of 1, 2, 3, 5 and 7 mtorr.

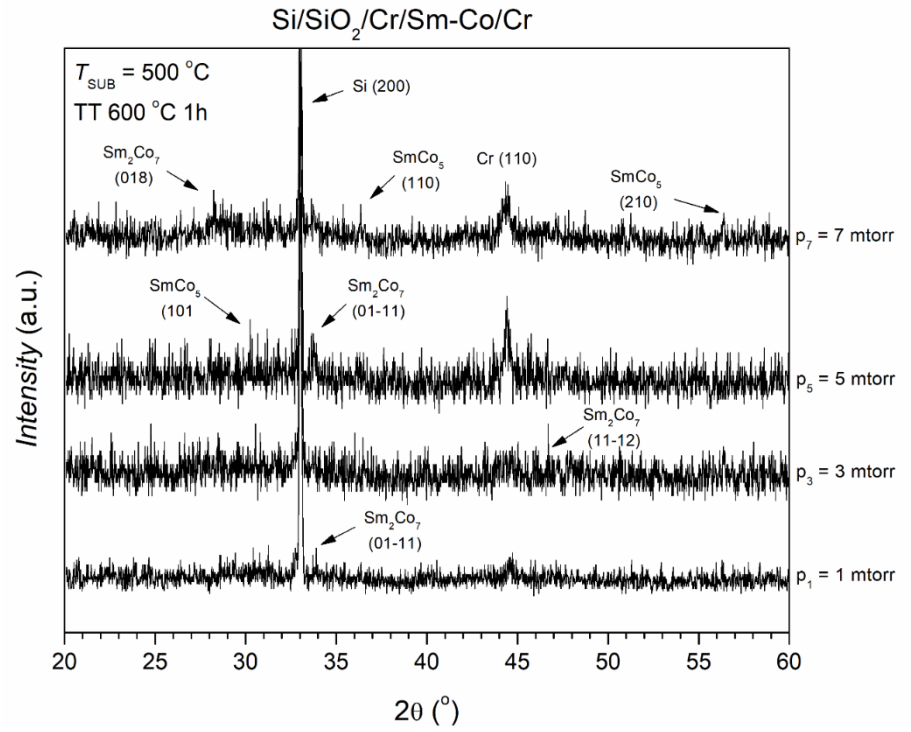


**Figure 5.** The X-ray diffraction patterns for the Cr/Sm-Co/Cr samples deposited on Si(100)/$SiO_2$ at substrate temperature 500 ºC and Ar pressures of 1, 2, 3, 5 and 7 mtorr, annealed at 600 ºC for 1h.

### 2.1.2. Effect of $Fe_{65}Co_{35}$ Thickness on the Magnetic Properties of Exchange Coupled Soft/Hard Cr/$SmCo_5$/$Fe_{65}Co_{35}$/$SmCo_5$/Cr Multilayers

Ferromagnetic (FM) thin films with strong out-of-plane magnetic anisotropy have been widely studied for perpendicular magnetic recording media applications [16, 17]. For this purpose, perpendicular anisotropy systems can be designed with high thermal stability to avoid superparamagnetic behavior [18] and with good writability [16], but this may raise the switching field above that which can be produced by currently available write heads. The use of tilted media, where the easy magnetization axis points at 45º to the film plane, has been proposed to reduce the switching field [19, 20], but the implementation of this method is complex. Considerable research has therefore been done on multilayer magnetic films where exchange coupling between dissimilar phases can be used to tailor the magnetic response. Perpendicular exchange coupled composite or exchange spring media have recently been introduced as candidate systems in which the magnetic response can be controlled. Perpendicular exchange spring systems consist of exchange-coupled hard and soft magnetic layers with respectively out-of-plane and in-plane easy magnetization axes. While the magnetically hard film provides thermal stability, the soft layer reduces the reversal field. When an external magnetic field is applied, the soft layer reverses first which creates an additional effective field applied to the hard phase through exchange coupling, lowering the switching field of the whole system. Modern permanent magnetic materials, like $SmCo_5$, are based on intermetallic compounds of rare-earth and 3*d* transition metals. Sm-Co intermetallics are hard magnetic materials with a high coercive field and a high uniaxial magnetocrystaline anisotropy, where the easy axis is aligned along the crystallographic *c*-axis.

An interesting and useful magnetic configuration is the combination between hard magnetic like $SmCo_5$ and soft magnets or superconductors. Such magnets are characterized by enhanced remanent magnetization and reversible demagnetization curves since the soft grains will rotate back into alignment with the hard grains when the applied field is removed. Coupled bilayer films provide convenient model systems for studying their properties because the relative length scales (e.g., thicknesses of the hard and soft magnet layers) can be controlled during the deposition process. In this section, we will investigate the effect of varying $Fe_{65}Co_{35}$ thickness on the magnetic properties of exchange coupled Cr/$SmCo_5$/$Fe_{65}Co_{35}$/$SmCo_5$/Cr multilayers.

Cr(100nm)/$SmCo_5$(50nm)/$Fe_{65}Co_{35}$(5-100nm)/$SmCo_5$(50 nm)/Cr(5 nm) configurations were deposited using DC magnetron sputtering on Si(100) substrates coated with 100 nm of $SiO_2$. The base pressure was better than $10^{-7}$ mbar. For the deposition of the Cr buffer layer,

the substrate was kept at room temperature, while the Ar pressure was kept at 3.5 mtorr and the sputtering power was 30 W. For the deposition of the $SmCo_5$ layers, the substrate temperature was kept at 500 ºC, while the Ar pressure was kept at 5 mtorr and the sputtering power was 90 W. The $Fe_{65}Co_{35}$ layer was deposited at 500 ºC, with an Ar pressure of 1.5 mtorr and a sputtering power of 30 W. The Cr capping layer was deposited at 500 ºC, using an Ar pressure of 3.5 mtorr and a sputtering power of 30 W. The layer thicknesses and deposition rates were monitored during the sputtering process using an Inficon SQM-160 rate/thickness monitor previously calibrated by X-ray reflectivity. The crystal structure of the prepared multilayers was investigated by X-ray diffraction using a Bruker D8 Advance diffractometer with Bragg-Brentano focusing geometry and Cu Kα radiation. The magnetic measurements were performed using a vibrating sample magnetometer with the field applied in-plane and out-of-plane, respectively, at 300 K in applied fields up to 4 T.

The X-ray diffraction patterns of the obtained multilayers is shown in Figure 6. All of the patterns contain a sharp peak around 33 degrees, which can be attributed to the Si(200) reflection of the substrate. Even though the Si(200) reflection is theoretically forbidden, it appears in our XRD patterns due to crystal damage which is induced when the substrates are cut. Another peak which was identified was the peak corresponding to the (110) reflection of the Cr substrate around 45 degrees, which is superimposed on the (110) reflection of the $Fe_{65}Co_{35}$ layer. The intensity of the Cr/$Fe_{65}Co_{35}$ peak increases with the $Fe_{65}Co_{35}$ thickness. From this we can infer that the films are textured along the (110)

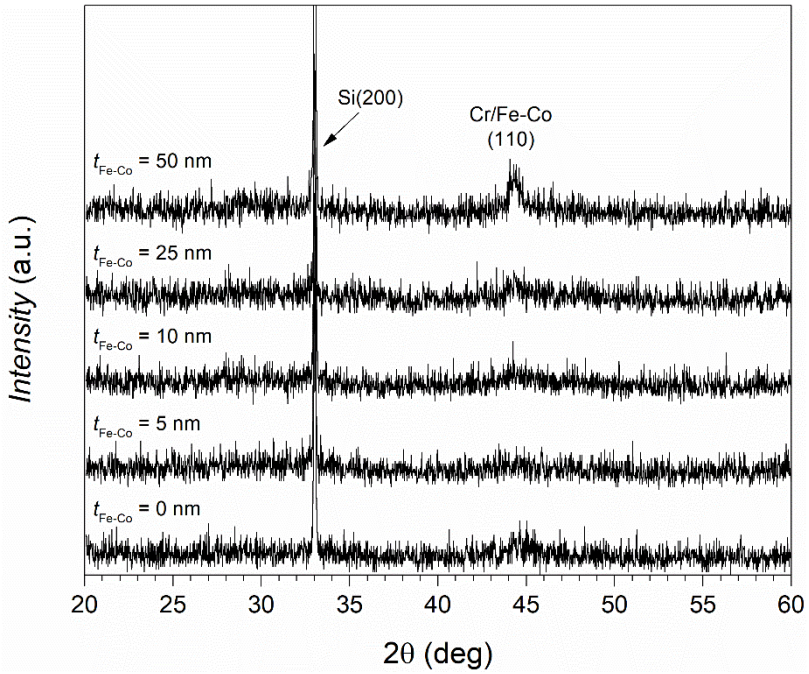


**Figure 6.** The X-ray diffraction patterns for the deposited Cr/$SmCo_5$/$Fe_{65}Co_{35}$/$SmCo_5$/Cr multilayers. The value $t_{Fe-Co}$ represents the $Fe_{65}Co_{35}$ layer thickness.

direction. No $SmCo_5$ reflections could be identified in the investigated 2θ range. The absence of the peaks could be attributed to the limitation of the powder XRD technique. The $SmCo_5$ layers each have a thickness of around 50 nm, which is below the detection limit of the powder diffraction technique, around 200 nm. However, the Cr and $Fe_{65}Co_{35}$ reflections were clearly identified. Due to the fact that both Cr and $Fe_{65}Co_{35}$ layers are textured along the (110) direction, and the first $SmCo_5$ layer is grown between these two layers, we can deduce that the $SmCo_5$ layer is crystalline and grows in tune with the Cr underlayer. As the mismatch between the lattice parameter of the (110) plane of Cr (4.08 Å) and the lattice parameter *c* of $SmCo_5$ (3.96 Å) is around 3%, we can assume that $SmCo_5$ layer grows along the *a*-axis of the $SmCo_5$ unit cell, i.e. the *c*-axis of $SmCo_5$ lies along the plane of the film – Figure 7.

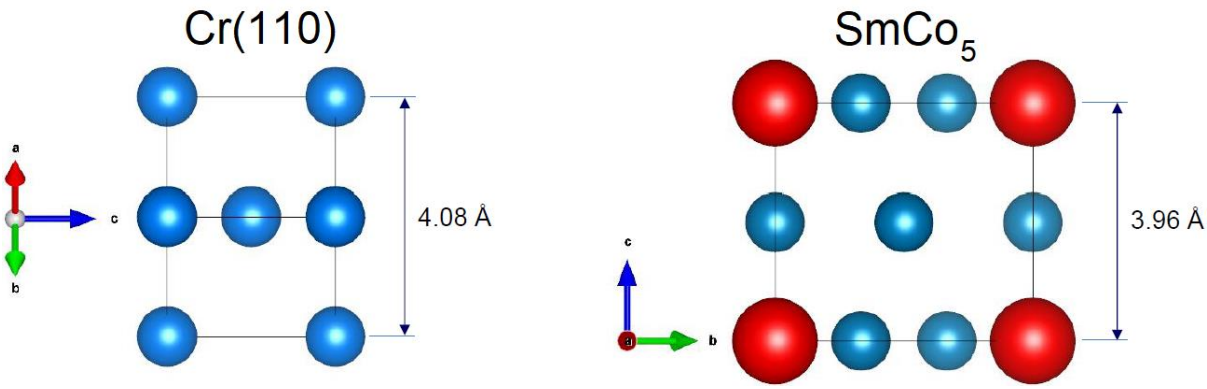


**Figure 7.** Illustration of the Cr and $SmCo_5$ unit cells.

The magnetic hysteresis loops measured with the field applied in-plane are shown in Figures 8a,b. It can be seen that the magnetization saturates quickly, in an applied field around 0.1 T – Figure 8a. Also, the saturation scales with the $Fe_{65}Co_{35}$ layer thickness, as

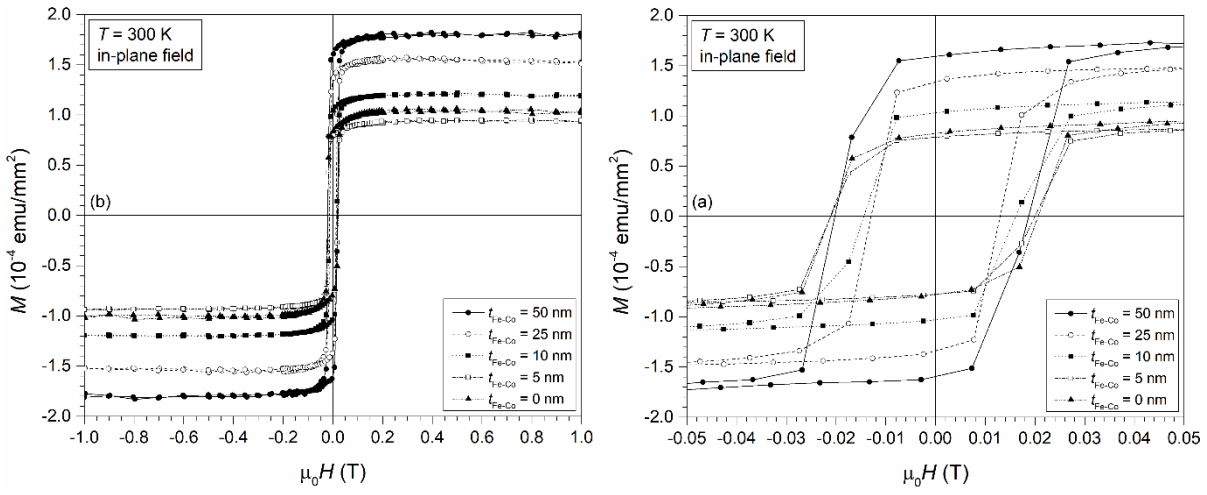


**Figure 8.** (a) Hysteresis loops measured at 300 K with the field applied in-plane between -1 and 1 T; (b) zoom-in on the same hysteresis loops between -0.05 and 0.05 T.

expected. The switching occurs in a narrow field range. Therefore, we can infer that the easy magnetization axis lies in the plane of the film. This also supports the hypothesis that the *c*-axis of $SmCo_5$, which is also its easy magnetization axis, lies along the plane of the film. The coercivity of the multilayers varies slowly around 0.02 T. The evolution of the coercivity versus $Fe_{65}Co_{35}$ thickness is discussed later in this section.

The hysteresis loops measured at 300 K with the field applied out-of-plane are shown in Figures 9a,b. We can observe that the magnetization saturates at a much higher field value than in the in-plane case, around 1.5 T. The saturation magnetization also scales with the thickness. However, the values are smaller than in the previous case of the field being applied in-plane. This can be attributed to the fact that the out-of-plane axis is the hard magnetization axis of the multilayers. Also, it is possible that the film magnetization is not fully rotated out-of-plane, which might explain the smaller saturation magnetization values. The coercive field values are slightly higher in the out-of-plane case than in the in-plane case, varying slowly around 0.03 T.

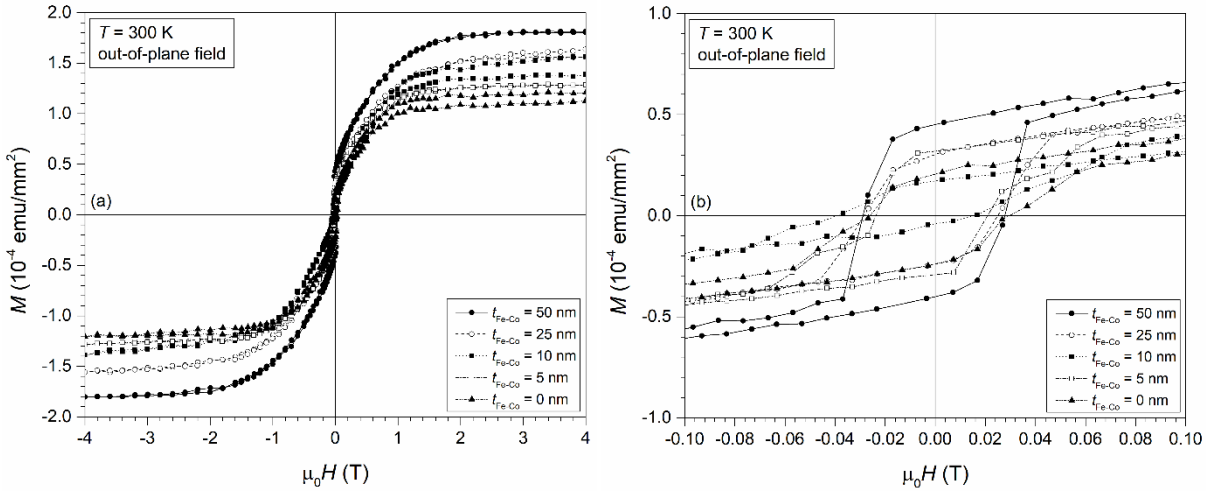


**Figure 9.** (a) Hysteresis loops measured at 300 K with the field applied out-of-plane between -4 and 4 T; (b) zoom-in on the same hysteresis loops between -0.1 and 0.1 T.

The evolution of the coercive field with the $Fe_{65}Co_{35}$ layer thickness is shown in Figure 10. For the in-plane case, the coercive field remains constant up to a $Fe_{65}Co_{35}$ thickness of 5 nm. For a $Fe_{65}Co_{35}$ thickness value of 10 nm the coercive field drops to 0.014 T and remains roughly constant up to 25 nm. At 50 nm the coercive field increases again to 0.02 T. For the out-of-plane case, the behavior is opposite the one obtained for the in-plane case. The coercive field initially decreases up to a $Fe_{65}Co_{35}$ thickness of 5 nm, after which it increases strongly to 0.039 T for 10 nm of $Fe_{65}Co_{35}$. If we increase the $Fe_{65}Co_{35}$ thickness even more, the coercivity drops and remains roughly constant at around 0.028 T. By analyzing this behavior, we can deduce that the optimum exchange coupling is obtained

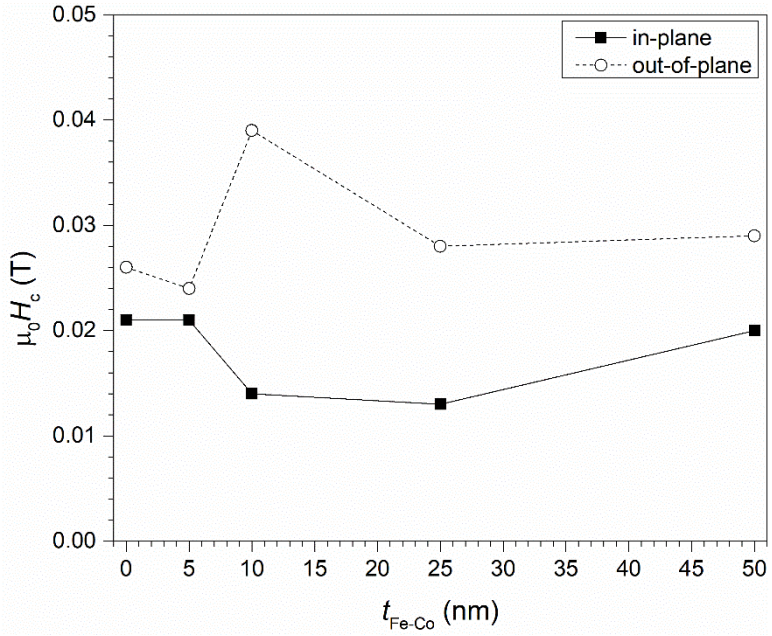


**Figure 10.** Coercive field values versus $Fe_{65}Co_{35}$ layer thickness obtained from hysteresis loops measured with the field applied in-plane and out-of-plane respectively.

for a $Fe_{65}Co_{35}$ thickness of 10 nm. By increasing the $Fe_{65}Co_{35}$ layer thickness the two layers become progressively uncoupled, at 50 nm of $Fe_{65}Co_{35}$ the coercivity being close to the case where there is no soft magnetic layer between the $SmCo_5$ layers.

## 2.2. Conclusions for Phase 3: January - September 2017

In Phase 3 we studied the effect of substrate type and deposition parameters (temperature, Ar pressure) on the structural properties of hard magnetic Cr/Sm-Co/Cr multilayers and the effect of $Fe_{65}Co_{35}$ thickness on the magnetic properties of exchange coupled hard/soft Cr/$SmCo_5$/$Fe_{65}Co_{35}$/$SmCo_5$/Cr multilayers.

It was shown that the complexity of the Sm-Co phase diagram can be triggered by varying the substrate type (Corning glass and Si/$SiO_2$) and deposition parameters (substrate temperature and Ar deposition pressure) of Cr/Sm-Co/Cr multilayers. For the multilayers deposited on Corning cover glass the Cr buffer layer was textured along the (110) direction. However, it has a reduced crystallinity which is transferred to the Sm-Co layer. It was found that the deposition pressure affects the stoichiometry of the Sm-Co layer, leading to various phase mixtures between $SmCo_5$ and $Sm_2Co_7$. It is worthwhile to note that no single $SmCo_5$ phase was obtained in the Sm-Co layers deposited on Cr/glass throughout the entire investigated pressure range. In the case of Cr/Sm-Co/Cr deposited on Si/$SiO_2$ substrates, the Cr underlayer is also textured along the (110) direction. As the pressure increases the Sm-Co layer is comprised of $SmCo_5$ and $Sm_2Co_7$ mixtures due to the fact that pressure affects stoichiometry, similarly to progressing through the Sm-Co phase diagram. A single

$SmCo_5$ phase was obtained at an Ar deposition pressure of 5 mtorr for both substrate temperatures (room temperature and 500 ºC). While a singular $SmCo_5$ was obtained for both substrate temperatures, a higher substrate temperature leads to a more intense and well-defined $SmCo_5$ peak due to the increased crystallinity of the Sm-Co layer. In both cases annealing leads to a decomposition of the Sm-Co phase into a mixture of $SmCo_5$ and $Sm_2Co_7$ phases.

The effect of varying $Fe_{65}Co_{35}$ layer thickness on the magnetic properties of $Cr/SmCo_5/Fe_{65}Co_{35}/SmCo_5/Cr$ multilayers was also studied. It was found that the multilayer films are textured along the (110) direction and that the *c*-axis of the $SmCo_5$ layers lies along the plane of the film. Magnetic measurements were performed with the field applied in-plane and out-of-plane respectively. For the in-plane field case, the magnetic switching occurred in a narrow field range, suggesting the fact that the easy magnetization axis lies along the plane of the film. For the out-of-plane field case, the magnetization saturated at a higher field value around 1.5 T, and its values were lower than the in-plane field case. This led us to believe that the out-of-plane film axis is the hard magnetization axis of the multilayers. Higher coercive field values were obtained for the out-of-plane field case than the in-plane field case, with the optimum exchange coupling being obtained for a $Fe_{65}Co_{35}$ thickness of 10 nm.

The results presented above show that both main project objectives have been accomplished, namely the preparation and study of hard and soft magnetic films and the study of exchange coupled multilayer systems. The results obtained through the activities outlined in the project were submitted for publication in ISI and BDI indexed articles [1, 2] and presented at international conferences [3-7]. A bachelor thesis was successfully completed on the project theme.

## 2.3. References for Phase 3: January - September 2017

[1] S. Mican, D. Benea, A. Takacs, O. Isnard, E. Mossang, V. Pop, *"Influence of Ferromagnetic Layer Thickness on the Exchange Bias in Cr/$Fe_{65}Co_{35}$ Bilayers"*, Paper submitted to Thin Solid Films - under review.

[2] R. Hirian, S. Mican, O. Isnard, L. Barbu, V. Pop, *"Effect of Starting Powder Premixing on the Interphase Exchange Coupling in $Nd_2Fe_{14}B$+10wt%Fe Nanocomposites Obtained Trough Mechanical Milling",* STUDIA UBB PHYSICA, Vol. 61 (LXI), 2, 2016, pp. 55-64.

[3] S. Mican, D. Benea, A. Takacs, O. Isnard, E. Mossang, V. Pop, *"Influence of Ferromagnetic Layer Thickness on the Exchange Bias in Cr/$Fe_{65}Co_{35}$ Bilayers"*, Oral

presentation at the 17th International Balkan Workshop on Applied Physics and Materials Science (IBWAP), 11th-14th July 2017, Constanţa, Romania.

[4] R. Hirian, S. Mican, O. Isnard, L. Barbu-Tudoran, V. Pop, *"Influence of Microstructure on the Interphase Exchange Coupling of $Nd_2Fe_{14}B$+10wt%α-Fe Nanocomposites Obtained at Different Milling Energies",* Oral presentation at the 2nd Poznań School of Physics of NanoMagnetism - POSNAMAG 2017, 21st-30th June 2017, Poznań, Poland.

[5] R. Hirian, O. Isnard, V. Pop, *"The influence of hard phase domain wall length on the magnetic behaviour of hard/soft exchange coupled nanocomposite powders obtained by mechanical milling"*, Oral presentation presented at the 5th International Conference on Powder Metallurgy & Advanced Materials, September 17th-20th, 2017, Cluj-Napoca, Romania.

[6] R. Hirian, T. Biter, A. Boiciuc, O. Isnard, V. Pop, *"Structural and magnetic behavior of the LTP MnBi phase"*, Poster presented at the European Conference Physics of Magnetism 2017 (PM'17), June 26th-30th, 2017, Poznań, Poland.

[7] R. Hirian, R. Gavrea, B. Neamţu, A. Ferenczi, O. Isnard, I. Chicinaș, V. Pop, *"Exchanged Coupled $SmCo_5$/α-Fe Nanocomposite Magnets Obtained by Mechanical Milling and Spark Plasma Sintering"*, Poster presented at the IEEE International Magnetics Conference (Intermag Europe) 2017, 24th-28th April 2017, Dublin, Ireland.

[8] A. Singh, V. Neu, S. Fähler, K. Nenkov, L. Schultz, and B. Holzapfel, Phys. Rev. B, [9] 77, 104443, 2008.

[10] Milton Ohring, T*he Materials Science of Thin Films*, Academic Press, New Jersey, 109-132, 1992.

[11] Y.C. Feng, D.E. Laughlin, D.N. Lambeth, Journal of Applied Physics, 76 (11), 7311, 1994.

[12] K. Buschow, A. van der Groot, *J. Less – Common Met*., 14, 323-328, 1968.

[13] S. Mican, *Magnetic Properties of 3d Transition Metals in Intermetallic Compounds and Oxides*, Teză de Doctorat, Universitatea Babeș-Bolyai, Cluj-Napoca, 2012.

[14] Y. Khan, *Zeitschrift Fur Metallkunde,* 65, 489-495, 1974.

[15] R. Downs, D. Palmer, *American Mineralogist,* 79, 9-14, 1994.

[16] H. J. Richter, J. Phys. D: Appl. Phys., 40, R149, 2007.

[17] J. H. Judy, J. Magn. Magn. Mater., 287, 16, 2005.

[18] D. Weller and A. Moser, IEEE Trans. Magn., 35, 4423, 1999.

[19] Z. K. Gao and H. N. Bertram, IEEE Trans. Magn., 38, 3675, 2002.

[20] J. P. Wang, Y. Y. Zhou,C. H. Hee, T. C. Chong and Y. F. Zheng, IEEE Trans. Magn.39, 1930, 2003.